

Hydration shell structure of the $\text{OH}^-(\text{H}_2\text{O})_{n=1-15}$ clusters from a model potential energy function

Alice Vegiri^{a)}

National Hellenic Research Foundation, Institute of Theoretical and Physical Chemistry,
48 Vas. Constantinou Av., Athens, 11 635 Greece

Sergei V. Shevkunov

Physics and Mechanics Department, St. Petersburg State Technical University, 29 Politekhnicheskaya ul.,
St. Petersburg, 195251 Russia

(Received 12 May 2000; accepted 25 August 2000)

The structural properties of the hydrated hydroxide ion are studied in terms of a many-body potential energy function that has been parameterized according to the experimentally determined [Arshadi *et al.*, J. Phys. Chem. **74**, 1475, 1483 (1970)] enthalpy and entropy changes for the first five association reactions of the ion with H_2O . Clusters in the $n=1-15$ size range are examined through a canonical Monte Carlo simulation at $T=297$ K. The resultant structures, irrespective of the cluster size, are predominantly linear of the dendrite type, with the first shell consisting of two water molecules. Minimum energy structures at $T=0$ K for $n=2$ and 3 compare well with *ab initio* conformations. © 2000 American Institute of Physics. [S0021-9606(00)51943-6]

I. INTRODUCTION

In previous work^{1,2} we examined the shell structure of protonated water clusters in terms of a model many-body potential energy function which had been simultaneously fitted to room temperature, experimental enthalpy and entropy changes^{3,4} resulting from the addition of one water molecule to the $(n-1)$ th cluster. In the current work we derive a similar model potential function for the $\text{OH}^-(\text{H}_2\text{O})_{n=1-15}$ clusters by utilizing corresponding incremental enthalpies and entropies measured by Kebarle and collaborators.^{5,6}

This specific approach, namely the exclusive utilization of *microscopic* rather than *macroscopic* thermodynamic data at room temperature for the generation of a potential function, is complementary to the approach used by other researchers, where potential models are constructed either through fitting to a number of *ab initio* points concerning the ion-water pair potential,^{7,8} or to *ab initio* minimum energy geometries of specific small ion-water clusters,⁹⁻¹² or to correlation functions and solvation enthalpies of the bulk,¹³ to name a few. Such potential functions have been extensively used for the study of the hydration properties of the alkali and halide ions in clusters or in solution.¹⁴⁻²³ However, the novelty of the current approach is the incorporation, for first time, of entropy information in the potential design. Usually potential models that are based on *ab initio* calculations are tested against experimental binding energies and not against free energies or entropies. Although enthalpy change gives a measure of the well depth for a single molecule attachment reaction, entropy gives a measure of the potential well shape and width through the density of states to which it is closely related.

This particular point has been raised by a few

authors^{24,25} who have pointed out that ion-water *ab initio* potentials or potentials that have been fitted to experimental gas-phase energies are rather inadequate for simulating the bulk phase, since their predicted solvation free energies differ considerably from the observed ones. In particular, Aqvist²⁵ has derived model potential functions for several ion-water systems by simultaneously fitting to bulk hydration free energies and ion-water oxygen radial-distribution-function peaks. The inclusion of three-body,²¹ rather than two-body, interactions was found to improve the agreement between the experimental and calculated solvation free energies, as the work by Kollman *et al.*²³ on the aqueous solutions of Li^+ and Na^+ ions indicates.

A systematic Monte Carlo (MC) study concerning the calculation of incremental enthalpies and free energies of small water clusters of single alkali metal and halide ions, and the comparison of these quantities with experiment, has been conducted by Mruzik and collaborators,²⁶ who have employed the Hartree-Fock (HF-SCF) potential energy surface by Kistenmacher *et al.*²⁷ for the corresponding ion-monohydrate system. These calculations have shown that the discrepancies between the MC and the experimental results increase with decreasing ion size, i.e., they are larger for Li^+ and F^- than for K^+ and Cl^- . Such a discrepancy is expected to exist for the hydroxide ion as well, which displays upon hydration similar enthalpy and entropy changes with cluster size as F^- , to which it is isoelectronic.

Also, Kollman and co-workers,²² by applying a three-body potential function,²¹ have calculated differential enthalpy and free energy changes between different clusters containing the same number of water molecules and different halide or alkali ions. By comparing the differential free energy results of Mruzik *et al.*,²⁶ which have been derived with pairwise-additive potentials on one hand, and those of Kollman *et al.*,²² which have been taken with many-body poten-

^{a)} Author to whom correspondence should be addressed. Electronic mail: avegiri@eie.gr

tials on the other hand, a significant overall improvement of the agreement with experiment, when nonadditivity is accounted for, is observed. However, when absolute free energy changes, ΔG , for the individual ions are considered, the agreement is found to vary from system to system (e.g., too bad for the K^+ ions and too good for the F^- ions).

The $OH^-(H_2O)_{n=1-15}$ clusters have attracted much less attention than their counterparts, the hydronium cations, despite their importance in atmospheric and biological processes. Experimental thermodynamic information about these clusters comes from the work of Kebarle and co-workers^{5,6} and Mautner and collaborators,²⁸ who are the only groups that have measured association enthalpies and entropies as a function of cluster size.

The $OH^-(H_2O)_n$ cluster distributions showing a weak, not always reproducible, magic number behavior at $n=11, 14, 17$, and 20 have also been generated in the laboratory by Castleman *et al.*²⁹ These clusters have been found to be less stable than the protonated ones and of different structural type.

There are several theoretical works,³⁰⁻³⁷ at different levels of approximation, which have investigated the energetics and structures of low energy conformations of the $OH^-(H_2O)_n$ clusters. Most of the work is devoted to the examination of structural and thermodynamic properties, like binding energies and enthalpies of the first three $n=1-3$ clusters. Gibbs free energies for cluster formation and free energy of solvation for the hydroxide ion at room temperature have been computed by Grimm and co-workers.³⁷ The behavior of the hydroxide ion in bulk has been examined by means of *ab initio* molecular dynamics.^{38,39} calculations, and in terms of an *ab initio* pairwise additive potential energy surface calculated for the OH^-H_2O pair.⁷

Unlike to the H_3O^+ ion, the proton in the OH^- monohydrate case, (HO^-H-OH) , is shared by the oxygen atoms by asymmetric hydrogen bonds,^{36,37} provided that the zero point energy is not considered.⁴⁰ The OH^- bond length in clusters does not differ much from the free case³² for all cluster sizes, whereas the water molecules can be safely considered as rigid for all sizes larger than $n=1$, if equilibrium properties are to be calculated.

Regarding the coordination of the hydroxide ion, theoretical studies in small clusters have shown that the water molecules attach to the oxygen site of the ion. Attempts to locate stable structures with one water molecule being hydrogen bonded to the hydrogen site of the ion have failed.^{33,37} Tri-, tetra-, and even penta-solvated³⁴ stable anionic clusters have been calculated, with the latter ones, however, being less energetically favorable than the tetra-coordinated. In fact, stable states with one water molecule attached to the hydrogen side of the ion have been found to exist for clusters equal to or larger than $n=17$,³⁴ provided that this extra molecule is constrained in position by several linear chains that make a link with the molecules of the first shell. Theoretical hydration numbers of the ion in the bulk have been found equal to 5.8 (Ref. 38) and 5.⁷ According to these calculations, the average structure in bulk consists of four⁷ or five³⁸ water molecules being hydrogen bonded to the oxygen atom of the ion, with one water molecule being tran-

siently or permanently attached to the hydrogen atom of it.

The solvation structure of the $OH^-(H_2O)_{n=1-15}$ clusters at room temperature is examined in the following sections. The description of the potential function and the presentation of the potential parameters are given in Sec. II. The hydration behavior of the anion and the resultant structures at room temperature are presented in Sec. III A. The location of minimum energy structures at $T=0$ and their comparison to *ab initio* ones from the literature are the subject of Sec. III B. Finally, Sec. IV summarizes and concludes.

II. POTENTIAL MODEL

The hydroxide ion OH^- is modeled in terms of three fractional charges, one screened negative charge Q_{sph} which is placed at the origin of the lab coordinate system, a second unscreened negative charge Q_{nsph} which is placed at the same position as Q_{sph} , and a third unscreened positive charge Q_H , which is placed along the positive z axis at a position equal to $d=0.967 \text{ \AA}$. The screening of the charges aims to the partial reduction of the directionality of the Coulomb interactions and to the enhancement of the covalent character of the bonds. The adopted fractional charge distribution for the OH^- ion corresponds to a dipole moment $\mu = 0.4053 \text{ a.u.}$, which is equal to the *ab initio* MCPF value of Ref. 41. Water-water interactions are described by the Stillinger-Rahman ST2⁴² pairwise-additive potential model. The water molecules and the OH^- ion are taken as rigid.

In the following, the separate terms that constitute the model potential function for a general ion-water system are presented.

The model consists of the following

(1) A term describing the ST2 pairwise additive water-water interactions: In the five centered Rahman and Stillinger ST2 potentials four charges of $q=1.132062 \times 10^{-10} \text{ cgs units}$, which are equal in magnitude, are placed on the vertices of a tetrahedron. The two positive and negative charges are located at a distance of 1.0 and 0.8 \AA , respectively, from the center occupied by the oxygen atom. In this model r_{OH} is equal to 1.0 \AA and the tetrahedral bond angle to $109^\circ 28'$.

The full potential between all pairs of water molecules is written as

$$U_{\text{pair}}^{w-w} = \sum_{i < j} \left\{ 4 \varepsilon_0^w \left(\left[\frac{\sigma^w}{r_{ij}} \right]^2 - \left[\frac{\sigma^w}{r_{ij}} \right]^6 \right) + s(r_{ij}) \sum_{k=1}^4 \sum_{l=1}^4 \frac{q_k q_l}{|\mathbf{r}'_k - \mathbf{r}'_l|} \right\}, \quad (1)$$

where ε_0^w and σ^w are equal to $5.2605 \times 10^{-15} \text{ erg}$ and 3.1 \AA , respectively.

Here $s(r_{ij})$ is an r -dependent screening function, introduced so as to smooth out the exaggerated heterogeneous electric field of the point charges,

$$s(r) = \begin{cases} 0, & < r < r_L, \\ (r - r_L)^2 (3r_U - r_L - 2r) / (r_U - r_L)^3, & r_L \leq r \leq r_U, \\ 1, & r_U < r < \infty, \end{cases} \quad (2)$$

TABLE I. Optimal potential parameters. *e* is the elementary charge.

$\sigma = 2.87 \text{ \AA}$	$\alpha_0 = 0.38110^{-12} \text{ erg}$	$Q_{sph} = -0.4691e$
$\epsilon_0 = 0.03110^{-12} \text{ erg}$	$b_0 = 15.25 \text{ \AA}$	$Q_{n sph} = -0.6343e$
$U_0 = 0.82710^{-12} \text{ erg}$	$m = 1.0$	$Q_H = 0.1034e$
$R_L = 4.94 \text{ \AA}$	$\tilde{R}_L = 3.23 \text{ \AA}$	
$R_U = 5.0 \text{ \AA}$	$\tilde{R}_U = 7.5 \text{ \AA}$	

with $r_L = 2.016 \text{ \AA}$ and $r_U = 3.1287 \text{ \AA}$.

Here r_k^i is the position vector of the *k*th point charge of the *i*th molecule and r_{ij} is the distance between any two Lennard-Jones centers. The singularities in the Coulombic potential are avoided by introducing spherical hard core potentials on each force center of the water molecule, so that for $r_{ij} < d_0 = 1.55 \text{ \AA}$ and $|\mathbf{r}_k^i - \mathbf{r}_l^j| < d_q = 0.1 \text{ \AA}$ the corresponding pair term becomes infinite.

(2) A term describing the water molecule polarization energy U_{pol}^w due to the electric field of the ion: For a single water molecule

$$u_{pol}^w(\mathbf{r}_0^i) = -\frac{1}{2}\alpha_w \mathbf{E}(\mathbf{r}_0^i)^2,$$

where

$$\mathbf{E}(\mathbf{r}_0^i) = \mathbf{E}^c(\mathbf{r}_0^i) + \sum_{l=1}^4 E_l^j(\mathbf{r}_0^i). \tag{3}$$

The summation is over all *k* ions in the system and *l* runs from 1 to 4 and denotes the point charges of the ion which correspond to the nonspherical part of the field. Here $\alpha_w = 1.44 \text{ \AA}^3$ is the experimental value of the isotropic polarizability of a single water molecule; \mathbf{r}_0^i is the coordinate vector of the geometric center of the *i*th water molecule; and $\mathbf{E}(\mathbf{r})$ represents the electric field of the ion, with $\mathbf{E}^c(\mathbf{r})$ and $E_l^j(\mathbf{r})$ denoting the spherical and nonspherical parts, respectively. A screening function $[s(R)]^2$, is applied only to the spherical part of the ionic field, where *s*(*R*) is the same as that of Eq. (2), but with different numerical values for the R_U and R_L parameters (see Table I). Here *R* is the distance from the ion to the oxygen atom of the molecule.

The total polarization energy U_{pol}^w is the summation of Eq. (3) over all water molecules in the cluster.

(3) Lennard-Jones terms between the oxygen atom of the ion and the water molecules: The Lennard-Jones potential parameters are listed in Table I.

(4) Coulomb interaction terms between all charges of the hydroxide ion and the point charges of the ST2 water molecules: As with polarization interactions, the spherical part of the ionic field is screened also by $[s(R)]^2$.

(5) A term modeling the nonelectrostatic, attractive interactions between the ion and the molecules: For a single water molecule

$$u_D(R_i) = -U_0[1 - s(R_i)], \tag{4}$$

where *s*(*R*) takes the same parameter values as in paragraph (2).

This term describes a simple flat potential that becomes equal to $-U_0$ for $R \leq R_L$ and equal to zero for $R \geq R_U$. The repulsive wall is set by the Lennard-Jones potential. Such a

potential well is dictated by the extreme flatness of the proton potential surface³⁶ in the ion-monohydrate case (H₃O₂⁻). For larger clusters, where protons are preferentially bonded to one oxygen atom, the flatness inserted by the $u_D(R)$ term is compensated by the repulsive many-body terms, which are described in the next paragraph.

(6) A term modeling the water-ion-water many-body interactions:

$$\tilde{U}^{ww} = \alpha_0 \left(\sum_{i < j} (\tilde{s}(R_i)\tilde{s}(R_j) \exp(-r_{ij}/b_0))^m \right)^{1/m}, \tag{5}$$

$$\tilde{s}(R) = \begin{cases} 1 & 0 < R < \tilde{R}_L, \\ 1 - (R - \tilde{R}_L)^2(3\tilde{R}_U - \tilde{R}_L - 2R)/(\tilde{R}_U - \tilde{R}_L)^3, & \tilde{R}_L \leq R \leq \tilde{R}_U, \\ 0, & \tilde{R}_U < R < \infty. \end{cases} \tag{6}$$

Here r_{ij} is the distance between any two water molecules and *R* is the ion-oxygen, water-oxygen distance. In the limiting case $m = 1$, expression (5) reduces to $\tilde{U}^{ww} = \alpha_0 \sum_{i < j} (\tilde{s}(R_i)\tilde{s}(R_j) \exp(-r_{ij}/b_0))$, which represents a three-body interaction for all $R \leq R_U$. For $m > 1$, the exponent $1/m$ in expression (5) allows for higher-order cross terms of the type $\dots[(\tilde{s}(R_i)\tilde{s}(R_j) \exp(-r_{ij}/b_0))[(\tilde{s}(R_k)\tilde{s}(R_l) \times \exp(-r_{kl}/b_0))\dots]$ to be included. The combination of the *m* and $1/m$ exponents facilitates the decomposition of the many-body interaction into a three-body interaction and into higher-order terms.

(7) Terms that describe the induced-dipole-induced-dipole interactions and the charge-induced-dipole interactions between all water molecules in the cluster: The total potential function results from the summation of terms 1–7.

The optimal potential parameters that reproduce the experimental consecutive enthalpies and free energies are listed in Table I.

Comparison between the experimental and calculated enthalpy, entropy, and free energy changes for the $n = 1 - 5$ clusters is in Table II.

Entropy change is extracted from the difference between enthalpy and free energy changes. In the current work, enthalpies of cluster formation have been calculated in the canonical ensemble, whereas free energies have been determined in the bicanonical statistical ensemble where only two states, consisting of *N* and *N* - 1 particles, are considered. The partition function and the method of sampling in this ensemble have been presented elsewhere.⁴³

In the current work the hydration structure of clusters with sizes in the $n = 1 - 15$ range and at $T = 297 \text{ K}$ have been examined. To avoid evaporation, the clusters remained confined in a spherical cavity with perfectly reflective walls of approximately 10 \AA in radius.

The calculated incremental entropies $-\Delta S_{n,n-1}$, free energies $-\Delta G_{n,n-1}$, and enthalpies $-\Delta H_{n,n-1}$ for a single molecule attachment and for $n = 1 - 5$ are illustrated in Fig. 1. In the same figure the corresponding experimental values by Kebarle *et al.*^{5,6} and Mautner *et al.*²⁸ are also displayed for comparison. These two are the only groups that have

TABLE II. Comparison of the calculated and experimental incremental enthalpies $\Delta H_{n-1,n}$ (kcal/mol), free energies $\Delta G_{n-1,n}$ (kcal/mol), and entropies $\Delta S_{n-1,n}$ (cal/(K.mol)).

$n-1,n$	Present work			Experimental data (Refs. 5 and 6)		
	$-\Delta H_{n-1,n}$	$-\Delta G_{n-1,n}$	$-\Delta S_{n-1,n}$	$-\Delta H_{n-1,n}^{\text{exp}}$	$-\Delta G_{n-1,n}^{\text{exp}}$	$-\Delta S_{n-1,n}^{\text{exp}}$
0,1	23.98	17.8	20.8	24	17.8	20.8
1,2	17.9	11.4	21.9	17.9	11.6	21.2
2,3	15.3	7.8	25.1	15.1	7.7	24.8
3,4	14.2	5.5	29.3	14.2	5.4	29.5
4,5	11.2	2.9	26.2	14.1	4.2	33.2

measured not only enthalpy but also sequential free energy changes. Although there is a satisfactory agreement between the experimental incremental enthalpies and entropies of cluster formation for cluster sizes less or equal than three, for larger clusters Mautner's data show considerably larger entropies and smaller binding energies.²⁸ Apart from that, Mautner's enthalpies show a break after $n=3$, a fact that points to the existence of a shell effect. Such an effect is not apparent in Kebarle's data. However, if the experimental errors in Mautner's data, of about 1 kcal/mol, are taken into account, then the existence of a first shell consisting of three water molecules at room temperature becomes questionable due to experimental uncertainties. The larger binding energies of Kebarle's $n=4$ and 5 clusters^{5,6} have been attributed by Mautner and collaborators to the possible existence of thermally dissociated ion clusters, a situation that is expected to be minimized in Mautner's experiments that have been conducted at lower temperatures.

In this work we have chosen Kebarle's experimental data for the calibration of the potential function. As seen from Fig. 1 and Table II, the coincidence of the first four theoretical and experimental entropies and enthalpies is exact. However, despite our efforts, we found it impossible to reproduce the experimental entropy and enthalpy of the fifth molecule attachment reaction. The respective fitted values turned out to be larger regarding entropy and smaller regarding enthalpy. In fact, the calculated enthalpy and entropy for

the fifth association reaction are close, within experimental error (1 kcal/mol for enthalpy and 2 cal/K.mol for entropy), to the respective Mautner's values.

III. RESULTS AND DISCUSSION

A. Structural properties at room temperature

Cluster equilibrium structures have been probed from ion-oxygen pair correlation functions calculated for $n=1-15$ and from water density distributions for specific cluster sizes. The results are displayed in Figs. 2 and 3, respectively.

Regarding the ion-oxygen correlation functions, a very well-defined hydration shell structure is observed, with the first, second, and third hydration shells peaking at about 2.5, 4.7, and 7.1 Å, respectively. Average hydration numbers for the first and second shells are displayed in Fig. 4. The information we get from these pictures is that the first shell, irrespective of the size of the cluster, consists of a constant average population of two water molecules, whereas the population of the second shell shifts from the value 3, for cluster sizes between $n=5$ and $n=9$, to the value 4, for clusters equal to $n=10$ and beyond. A third shell appears at a cluster size equal to $n=6$ and before the second shell has been completed.

Representative Monte Carlo configurations with a tri- and a tetra-coordinated second shell are displayed in Figs. 5(b) and 5(a) respectively. According to this picture the configurations, irrespective of the cluster size, are generated out

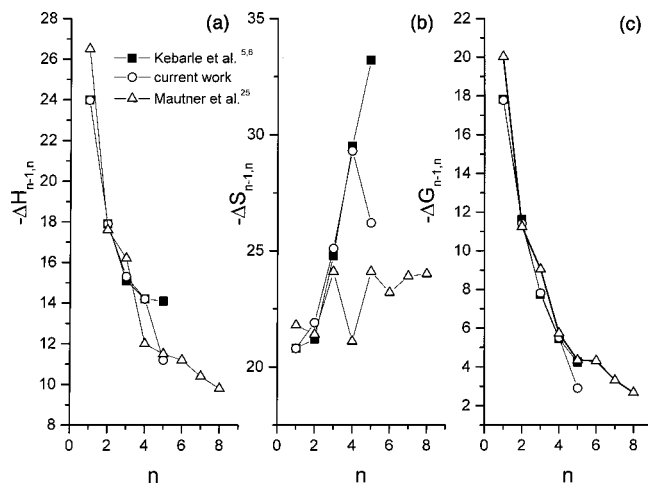


FIG. 1. Comparison of current work with experiment: (a) enthalpy changes, $-\Delta H_{n-1,n}$ as a function of cluster size n in kcal/mol, (b) entropy changes, $-\Delta S_{n-1,n}$ in cal/mol/K and (c) free energy changes, $-\Delta G_{n-1,n}$ in kcal/mol.

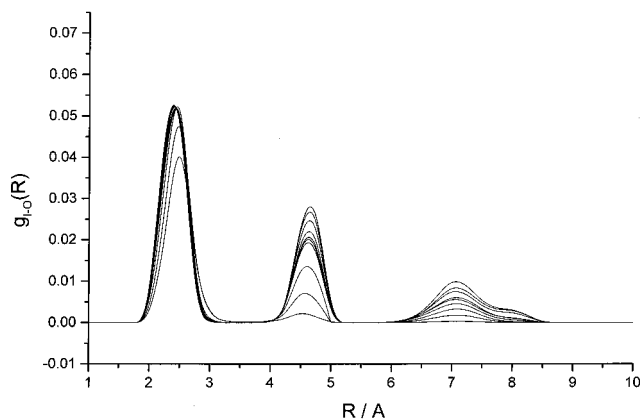


FIG. 2. Ion oxygen-water oxygen pair correlation functions in Å^{-3} for $n=2-15$.

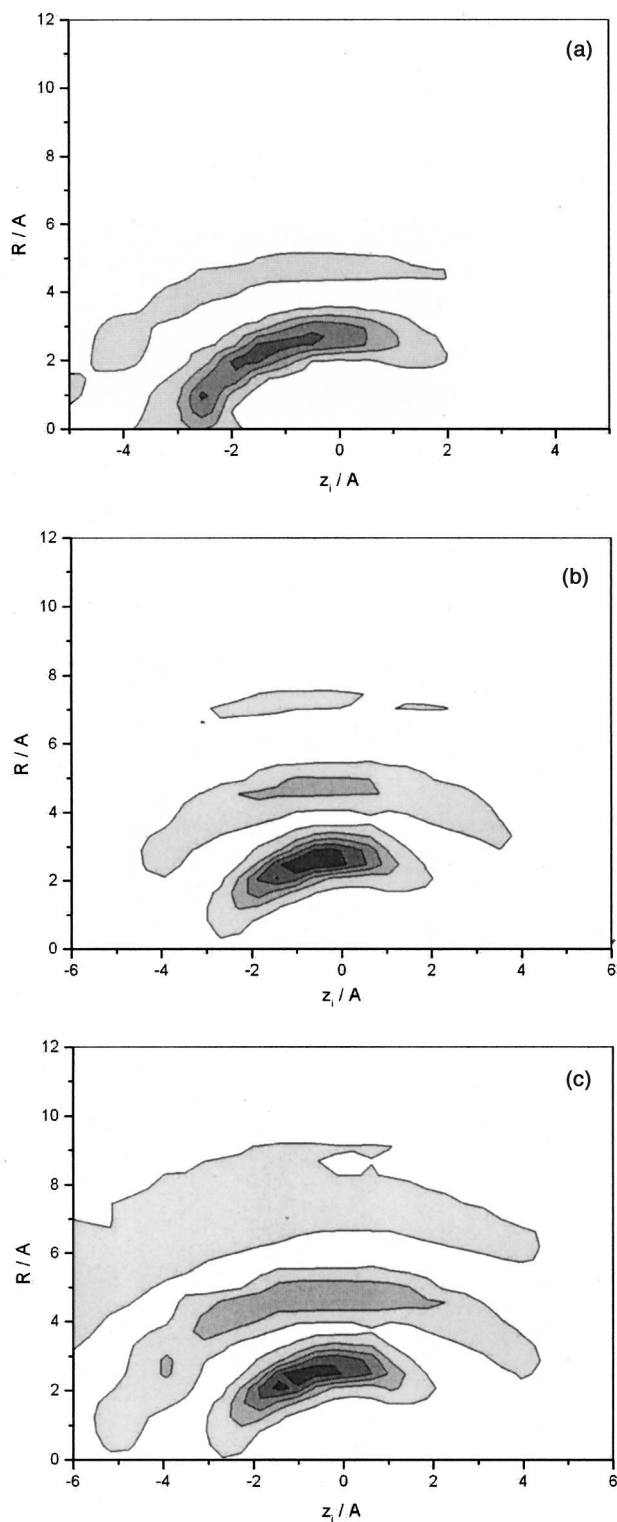


FIG. 3. Water molecule density distributions as a function of the cylindrical coordinates R and z_i , for the (a) $n=3$, (b) $n=6$, and (c) $n=10$ clusters.

of a central H_5O_3^- structural unit, which evolves according to a dendrite-type pattern. The general scheme is that the two molecules of the first shell act as proton donors to the oxygen atom of the hydroxide ion. In a chainlike fashion, the molecules of the second shell act similarly as proton donors to the molecules of the first shell and so on. The picture of a doubly coordinated hydroxide ion is also substantiated by

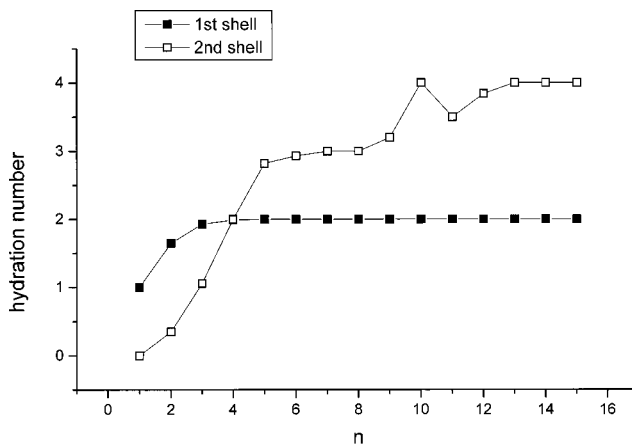


FIG. 4. First and second shell coordination numbers as a function of cluster size.

preliminary fits to the Mautner *et al.*²⁸ experimental enthalpy and entropy data.

The hydration of the hydroxide ion in the bulk has been studied by Andaloro *et al.*⁷ by employing an *ab initio* (SCF LCAO) pair potential for the ion-water complex and by *ab initio* molecular dynamics calculations by Tuckerman *et al.*^{38,39} In the former case, average configurations consisting of five water molecules in the immediate vicinity of the ion, four of which being hydrogen bonded to the oxygen atom of the ion, have been located. In the latter case, the hydroxide anion has been found to coordinate with as many as 5.8 water molecules. Four of them have been found to be almost coplanar, forming in this way the base of a pyramid

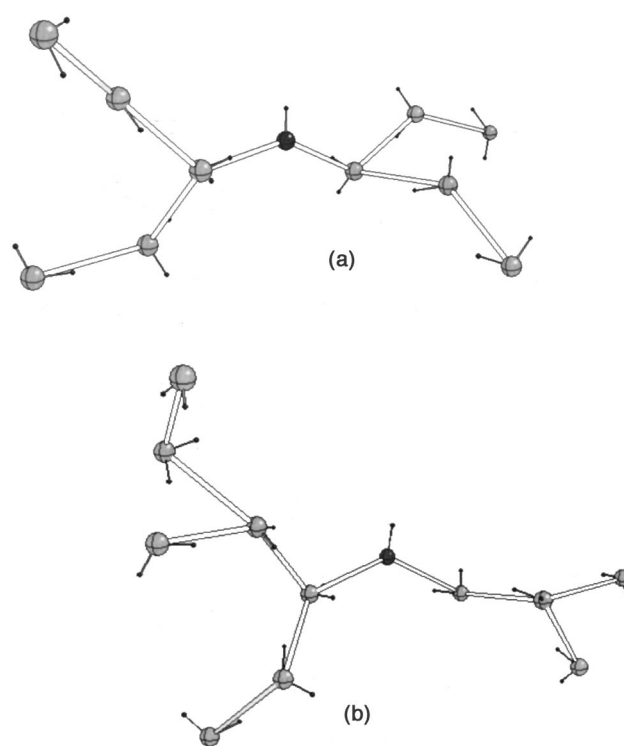


FIG. 5. Monte Carlo representative configurations with a (a) tetra- and a (b) tri-coordinated second shell.

with the oxygen atom of the ion on its apex, with the remaining two ligands being involved in transient bonds with the hydrogen and oxygen atoms of the ion above and below the pyramidal plane.

Regarding the hydration structure of the ion, there is a discrepancy between our results and the previous calculations. The major component of the discrepancy can be attributed to the inclusion of entropy information in the construction of the present potential function, a factor that is absent from the aforementioned potentials. Molecular conformations at temperatures other than zero are generated according to the minimum of the free energy rather than the minimum of the potential energy surface. Cluster structures that are based on a tetra-coordinated anion are more favorable on energetic grounds, since the four water molecules tend to benefit the most from their vicinity with the stronger ionic field. On the other hand, structures that tend to sacrifice their binding energy in favor of entropy, i.e., from the increase of their entropic content, prefer to take up more open forms, like the linear conformations observed in the current model.

There are also a few more facts that should be taken into account. First, the larger hydration numbers of the previous simulations refer to the coordination of the ion in the bulk liquid, and not to the coordination of it in small clusters in gas phase, as the current work does. The simple extrapolation of the hydration behavior of an ion in a cluster environment to that it would have had in bulk is not always straightforward. If we take as an example the much-studied solvation of the Cl^- ion in water,¹⁹ we find a change of structure from internal to surface states, and a concomitant decrease of the coordination number, as the number of water molecules in the cluster increases.

Second, linear isomers with shells consisting of two water molecules have also been proposed by Mautner and collaborators in order to explain the shell effect observed in their experimental data.

Finally, we can refer to the solvation structures of water clusters in the presence of an electron. Evidence for linear chains of negatively charged small water clusters with a size between $n=5$ and $n=11$ has been recently given by IR spectroscopic means,⁴⁴ without these chainlike structures being energetically the most stable forms of the anionic water clusters.^{45,46}

Unfortunately, no x-ray or neutron scattering experiments or spectroscopic data exist that could give an estimate of the hydration structure of the particular hydroxide ion in bulk or in individual clusters at room temperature.

As far as the spatial arrangement of the solvent molecules around the ion is concerned, this is shown on the density plots of Fig. 3. Figures 3(a)–3(c) are for $n=3$, $n=6$, and $n=10$ water molecules, respectively. Density distributions are calculated in terms of the cylindrical R and z coordinates on z_i planes perpendicular to the z axis. We note that the hydrogen atom of the hydroxide ion lies on the positive z axis at a distance $d=0.967 \text{ \AA}$ from the origin, which in turn is occupied by the oxygen atom of the ion. The water molecules of the first shell are most probably arranged around the oxygen side of the ion with the hydrogen atom pointing away from the cluster. This structural preference is

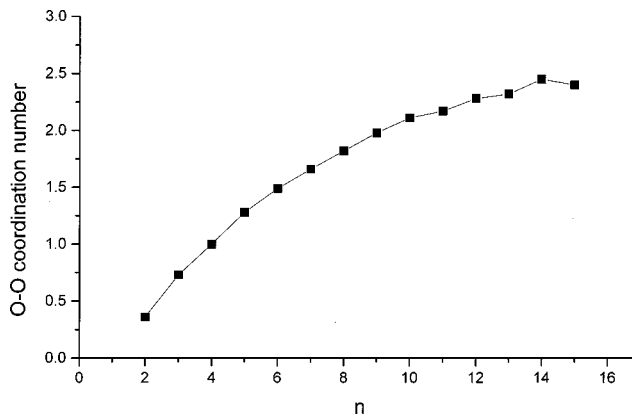


FIG. 6. Oxygen–oxygen coordination numbers as a function of cluster size.

also confirmed from spectroscopic studies of aqueous alkali metal hydroxides^{47,48} in bulk, which show that OH^- is bonded to the water molecules with its oxygen atom rather than with its hydrogen. In a similar fashion, the negative z axis for the larger clusters is also free of molecules [see Figs. 3(b) and 3(c)].

The structure of water molecules surrounding the ion is probed by the water molecule oxygen–oxygen pair correlation function. Oxygen–oxygen coordination numbers ($n_{\text{o-o}}$) for the $n=1-15$ clusters are displayed in Fig. 6. For the $n=3$ cluster $n_{\text{o-o}}$ is equal to 0.73, which indicates that the majority ($\sim 90\%$) of the equilibrium configurations at room temperature are linear and the rest (10%) are of the ring type. A ring structural unit consists of two water molecules directly bonded to the ion with the third one acting as a double donor to the other two. The above percentage of the configuration types is derived if we take into account that the first shell of the ion consists of two water molecules only and that the average coordination numbers of a water molecule in the doubly coordinated linear and ring configurations for $n=3$ are equal to 0.67 and 1.33, respectively. The ring structures therefore are responsible for the water density that appears on the negative z axis for the $n=3$ clusters in Fig. 3(a).

For the $n=4$ cluster, $n_{\text{o-o}}=1.0$, a value that leaves no doubt about the nature of the configurations which are exclusively of the linear type, with the hydroxide ion occupying the center of the chain. For the $n=5$ clusters, $n_{\text{o-o}}=1.28$, which implies similar linear configurations as for the $n=4$ case, but with the extra fifth molecule attached to the second ionic shell. Such a configuration gives a mean coordination number equal to 1.2 and is consistent with the occupation of the second ion shell by three water molecules as shown in Fig. 4.

B. Low energy structures at $T=0$

In the following, low energy structures for the $n=2-4$ clusters generated through quenching of various molecular dynamics trajectories at periodic time intervals are compared to *ab initio* conformations³²⁻³⁷ as they appear in the literature. One thing we should keep in mind is that it is not possible to make a direct comparison for the following reasons. The model potential is based exclusively on room tem-

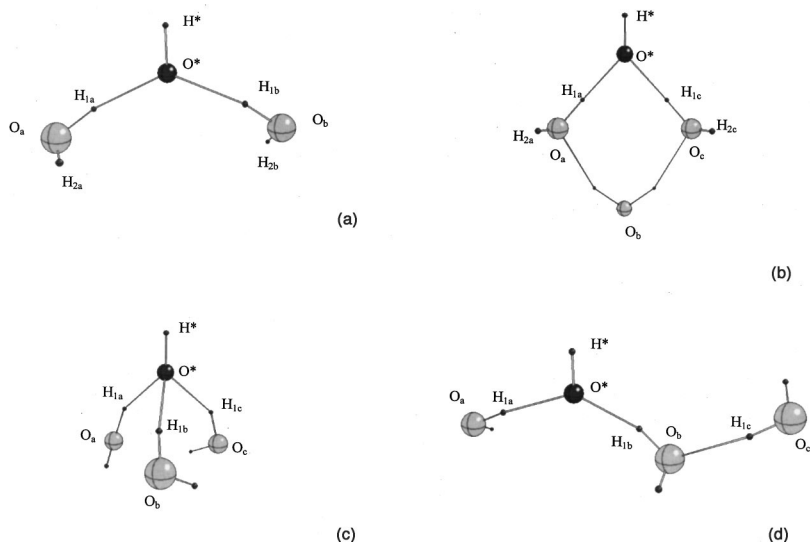


FIG. 7. Minimum energy structures for the $n=2$ and $n=3$ clusters.

perature thermodynamic data where thermal and quantum fluctuations of the clusters are inherently taken into account. This kind of information is absent from the *ab initio* structures which are calculated at $T=0$ K. Therefore the expected discrepancies between the current and the *ab initio* minimum energy structures will originate from uncertainties in bond angles and bond lengths, at least of the order of the de Broglie wavelength. A rough estimate of the spatial delocalization $\Delta = \sqrt{\hbar/\mu\omega}$ of the quantum $\text{OH}^-(\text{H}_2\text{O})$ system can be

obtained if we substitute for μ the reduced mass of it and for ω the symmetric hydrogen-bonded stretching vibration of about 300 cm^{-1} .³² This provides a value of about 0.1 \AA for Δ . A second reason is the assumption of rigid water molecules, which, although the assumption poses no problems to the prediction of equilibrium structures, it is significant for the direct comparison of the geometrical parameters of the minimum energy structures because of the distortions the water molecules that are taking part in the ion-molecule hy-

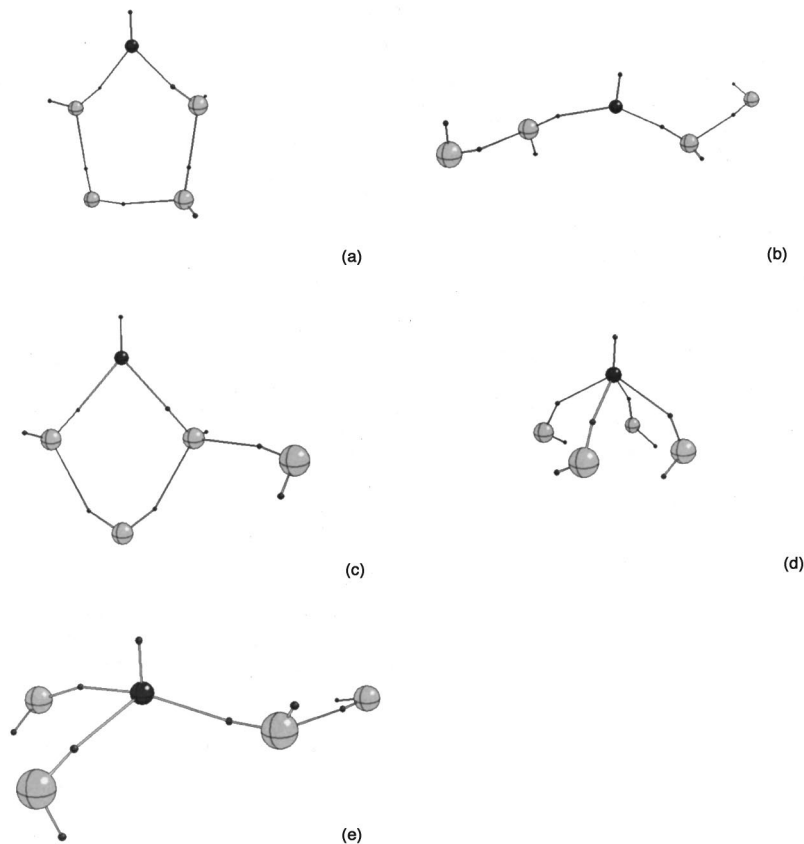


FIG. 8. Minimum energy structures for the $n=4$ clusters.

TABLE III. Internal coordinates for the minimum energy structure of the OH⁻(H₂O)₂ cluster. The oxygen and hydrogen atoms of the ion are distinguished by (*). Distance in a₀.

	Present work	Xantheas (Ref. 32)	Wei <i>et al.</i> (Ref. 36)	Turki <i>et al.</i> (Ref. 35)	Grimm <i>et al.</i> (Ref. 37)
O*O _a	5.05	4.87	4.91	4.99	4.87
(O _a Ô*O _b)	124.3°	115.6°	128.3°	80.9°	
O _a O _b	8.9	8.27	8.85		
O*H _{1a}	3.27	2.91	2.95		2.9
(O*H _{1a} O _{1a})	155.3°	176°			174°
(H*Ô*H _a)	113.8°	108.5°			

drogen bond are experiencing. Namely, a significant elongation of the proton-donor to the ion molecular bond has been calculated.³⁵

Low energy structures are displayed in Fig. 7 for the $n=2$ and 3 clusters and in Fig. 8 for $n=4$. The structures are presented in increasing energy in going from left to right and from top to bottom. Figures 7(b)–7(d) represent the ring, pyramidal, and linear conformations of the $n=3$ cluster.

The geometries of the OH⁻(H₂O)₂ cluster and of the pyramidal, *cis*-ring, and linear structures of OH⁻(H₂O)₃ from the current potential are compared to the respective *ab initio* structures that are available in the literature in Tables III and IVa–c.

Two types, similar in geometry ring structures, have been found, the *cis*- and *trans*-ones, with the H_{2a} and H_{2c} free hydrogens being at *cis*- and *trans*-relative positions, respectively.

The internal geometrical parameters and energies of Xantheas³² $n=2$ and 3 clusters that are displayed in the aforementioned tables correspond to the MP2/aug-cc-pVDZ level of theory. Those of Wei *et al.*³⁶ correspond to the DFT/PLAP3/Sadlej-basis computational scheme, those of Turki *et al.*³⁵ correspond to MP2 calculations with constrained intramolecular geometries, those of Tuñón *et al.*³³ to the HF/6-31+G* level, and finally those by Grimm *et al.*³⁷ correspond to the MP2/DZP(s,p) scheme.

Regarding the geometry of the OH⁻(H₂O)₂ cluster (Table III), which as we have seen represents the basic structural unit of all larger clusters, is almost identical to the DFT geometry of Wei *et al.*³⁶ if the O_aO*O_c frame is considered (see Table III for the O_aO_b and O*O_a distances and the O_aÔ*O_b angle). The model ring and pyramidal minimum energy structures of the OH⁻(H₂O)₃ cluster (Tables IVa and b) are closer to those of Xantheas,³² with the current pyramidal structure being somewhat more compressed. In contrast to the Wei *et al.*³⁶ pyramidal structures, which are significantly more open, the Xantheas³² and current structures

TABLE IV. Internal coordinates for the (a) ring, (b) pyramidal, and (c) linear structures of the OH⁻(H₂O)₃ cluster. The oxygen and hydrogen atoms of the ion are distinguished by (*). Distance in a₀.

	Present work	Xantheas (Ref. 32)	Tuñón <i>et al.</i> (Ref. 33)	Wei <i>et al.</i> (Ref. 36)	Grimm <i>et al.</i> (Ref. 37)
Ring structure					
O*O _a	5.05	4.83			
(O _a Ô*O _c)	41.5°	51.5°			
O _a O _b	5.46	5.49			
O*H _{1a}	3.23	2.86	3.09		
(H*Ô*H _{1a})	134.5°	111.3°	115.6°		
Pyramidal structure					
O*O _a	5.1	4.97		5.03	5.02
(O _a Ô*O _c)	64.6°	78.1°		125.2°	
O _a O _b	5.46	6.27		8.9	
O*H _{1a}	3.4	3.13	3.26	3.15	3.1
(O*Ô*H _{1a})	131.0°	127.0°	116.0°		
Linear structure					
O*H _{1a}	3.27		3.21		
(O _a Ô*O _c)	126.8°		136.1		
(O*Ô _b O _c)	125.6°		128.9°		

have the water molecules of the basis of the pyramid bonded in a cyclic way. Finally, the present linear structure is very close to that of Tuñón *et al.*³³ (Table IVc).

Despite the fact that the proposed potential model can reproduce the framework of the structure consisting of the atomic oxygens, it fails to reproduce the *ab initio* linearity of the hydrogen bonds (~175°) between the water molecules and the ion. Instead, the hydrogen bonds have been found to be nonlinear at about 155°. The consequence of this is that the hydrogen bonds (O*--H_{1a}) of the current model are significantly longer than the *ab initio* values. We believe that this is probably related to the specific potential model (ST2) we have adopted for the water–water interactions with the pronounced bond directionality.

In Table V, the first three association enthalpies calculated with the current potential are compared with the *ab initio*^{32,36,37} and the experimental^{5,6} values. Wei *et al.*³⁶ and Grimm *et al.*³⁷ enthalpies are closer to the experimental values than those of Xantheas,³² which are systematically overestimated by about 2 kcal/mol.

Similarly in Table VI, the first three free energy and entropy changes calculated with the current potential function are compared with the *ab initio* values of Grimm *et al.*³⁷ and the experiment.^{5,6} In fact, the Grimm *et al.*³⁷ values are much closer to the revised experimental free energies and entropies⁶ than to the older ones⁵ to which they are compared in Ref. 37.

TABLE V. Association enthalpies $\Delta H_{n-1,n}$ (298 K) in kcal/mol.

$\Delta H_{n-1,n}$ (298 K)	Present work	Wei <i>et al.</i> (Ref. 36)	Xantheas (Ref. 32)	Grimm <i>et al.</i> (Ref. 37)	Expt. (Refs. 5 and 6)
OH ⁻ (H ₂ O) _{0,1}	-23.98	-24.5	-27.8	-25.1	-24.0
OH ⁻ (H ₂ O) _{1,2}	-17.9	-17.9	-20.1	-18.4	-17.9
OH ⁻ (H ₂ O) _{2,3}	-15.3	-14.4	-16.9	-15.2	-15.1

TABLE VI. $\Delta G_{n-1,n}(298\text{ K})$ in kcal/mol and $\Delta S_{n-1,n}(298\text{ K})$ in cal/(K mol).

	$-\Delta G_{n-1,n}(298\text{ K})$			$-\Delta S_{n-1,n}(298\text{ K})$		
	Present work	Grimm <i>et al.</i> (Ref. 37)	Expt. (Refs. 5 and 6)	Present work	Grimm <i>et al.</i> (Ref. 37)	Expt. (Refs. 5 and 6)
$\text{OH}^-(\text{H}_2\text{O})_{0,1}$	17.8	17.7	17.8	20.8	24.7	20.8
$\text{OH}^-(\text{H}_2\text{O})_{1,2}$	11.4	10.7	11.6	21.9	26.0	21.2
$\text{OH}^-(\text{H}_2\text{O})_{2,3}$	7.8	6.9 (pyramidal)	7.7	25.1	27.8 (pyramidal)	24.8

Regarding the energy ordering of the minimum energy structures of the $\text{OH}^-(\text{H}_2\text{O})_3$ cluster, it has been found³² that the pyramidal and ring ones differ by 1.15 kcal/mol in electronic energy and by 0.6 kcal/mol if zero-point energy corrections are included. Although the pyramidal structure is the most stable of the two, both of them can be equally accessible at room temperature. The current model predicts the *trans*-ring structure as the minimum energy structure. The *cis*-ring structure has been found to lie higher in energy, by 0.27 kcal/mol, with the pyramidal and linear structures at 0.3 and 1.52 kcal/mol, respectively. Although the *ab initio* ordering of the ring and pyramidal structures is not reproduced by the current model, their energy difference, however, is not far from the *ab initio* energy range.

Regarding the minimum energy conformations of the $\text{OH}^-(\text{H}_2\text{O})_4$ cluster (Fig. 8), those with the lowest energy are the structures with the doubly coordinated hydroxide ion, in Figs. 8(a)–8(c) with energies at 0.0, 1.98, and 2.06 kcal/mol, respectively. Next in energy, at 3.4 kcal/mol, is the four-coordinated pyramid [Fig. 8(d)] and very close to it, at 3.65 kcal/mol, comes the tri-coordinated ion with the fourth water molecule in the second shell [Fig. 8(e)].

IV. SUMMARY AND CONCLUSIONS

In the present study we have constructed a model many-body potential energy function, based on experimental^{5,6} thermodynamic data concerning the first five incremental enthalpy and entropy changes from the hydroxide ion hydration reactions. This is an alternative approach to the DFT^{38,39} and pairwise additive SCF⁷ potential energy surfaces employed so far for the examination of the structural properties and dynamics of the same system. As far as we know, this is the first time that entropy information is incorporated in an explicit way into the construction of a potential energy function.

This potential surface has been used for the investigation of the equilibrium structures of the $n=1-15$ clusters at room temperature through a series of MC simulations. The main results are that (a) the solvation number is equal to two for all cluster sizes examined, (b) the most frequently met configurations are bifurcated linear chains ordered in a dendrite-type fashion, and (c) the water molecules attach to the oxygen site of the ion. More specifically, the $n=3$ clusters at room temperature are 90% linear and 10% of the ring type. The $n=4$ clusters are exclusively linear (two molecules in each shell) with the hydroxide ion occupying the center of the chain. The $n=5$ clusters are also linear with two and three molecules in the first and second shells, respectively.

The preference of these clusters to be organized in entropy-rich linear chains rather than in energy-poor tri- and tetra-coordinated structures can be understood in terms of the minima not of the potential energy but of the free energy surface of these systems.

Minimum energy structures which have been generated for the $n=2-4$ clusters compare well with the respective *ab initio* structures within the bond length deBroglie uncertainties.

In this work, we present a portable potential energy function for the description of small $\text{OH}^-(\text{H}_2\text{O})_n$ clusters. This function reproduces exactly the experimental^{5,6} enthalpy and entropy changes. In addition, it has been tested against a number of *ab initio* geometries of minimum energy configurations, with very good performance. All these facts increase our confidence about the reliability of the structural results that we get out of this function for clusters at room temperature. A further crucial test would have been its application to the calculation of the solvation free energy of the hydroxide ion in bulk. We intend to undertake such a task in the near future.

ACKNOWLEDGMENTS

Financial support by the CRG.LG-973972 and the PST.CNS-975408 NATO grants is gratefully acknowledged.

- S. V. Shevkunov and A. Vegiri, J. Chem. Phys. **111**, 9303 (1999).
- S. V. Shevkunov and A. Vegiri, Mol. Phys. **98**, 149 (2000).
- A. J. Cunningham, J. D. Payzant, and P. Kebarle, J. Am. Chem. Soc. **94**, 7627 (1972).
- Y. K. Lau, S. Ikuta, and P. Kebarle, J. Am. Chem. Soc. **104**, 1462 (1982).
- M. Arshadi and P. Kebarle, J. Phys. Chem. **74**, 1483 (1970).
- J. D. Payzant, R. Yamdagni, and P. Kebarle, Can. J. Chem. **49**, 3308 (1971).
- G. Andaloro, M. A. Palazzo, M. Migliore, and S. L. Fornili, Chem. Phys. Lett. **149**, 201 (1988).
- S. L. Fornili, M. Migliore, and M. A. Palazzo, Chem. Phys. Lett. **125**, 419 (1986).
- J. Caldwell, L. X. Dang, and P. A. Kollman, J. Am. Chem. Soc. **112**, 9144 (1990).
- L. X. Dang, J. E. Rice, J. Caldwell, and P. A. Kollman, J. Am. Chem. Soc. **113**, 2481 (1990).
- L. X. Dang, J. Chem. Phys. **96**, 6970 (1992).
- J. Chandrasekhar, D. C. Spellmeyer, and W. L. Jorgensen, J. Am. Chem. Soc. **106**, 903 (1984).
- S. J. Stuart and B. J. Berne, J. Phys. Chem. **100**, 11934 (1996).
- L. Perera and M. L. Berkowitz, J. Chem. Phys. **96**, 8288 (1992).
- L. Perera and M. L. Berkowitz, J. Chem. Phys. **95**, 1954 (1991).
- L. X. Dang and D. E. Smith, J. Chem. Phys. **99**, 6950 (1993).
- W. L. Jorgensen and D. L. Severance, J. Chem. Phys. **99**, 4233 (1993).
- L. X. Dang and B. C. Garrett, J. Chem. Phys. **99**, 2972 (1993).
- I. C. Yeh, L. Perera, and M. L. Berkowitz, Chem. Phys. Lett. **264**, 31 (1997).
- L. Perera and M. L. Berkowitz, J. Chem. Phys. **99**, 4222 (1993).

- ²¹T. P. Lybrand and P. A. Kollman, *J. Chem. Phys.* **83**, 2923 (1985).
- ²²P. Cieplak, T. P. Lybrand, and P. A. Kollman, *J. Chem. Phys.* **86**, 6393 (1987).
- ²³P. Cieplak and P. A. Kollman, *J. Chem. Phys.* **92**, 6761 (1990).
- ²⁴M. Migliore, G. Corongiu, E. Clementi, and G. C. Lie, *J. Chem. Phys.* **88**, 7766 (1988).
- ²⁵J. Aqvist, *J. Phys. Chem.* **94**, 8021 (1990).
- ²⁶M. R. Mruzik, F. F. Abraham, and D. E. Schreiber, *J. Chem. Phys.* **64**, 481 (1976).
- ²⁷H. Kistenmacher, H. Popkie, and E. Clementi, *J. Chem. Phys.* **59**, 5842 (1973).
- ²⁸M. Mautner and C. V. Speller, *J. Phys. Chem.* **90**, 6616 (1986).
- ²⁹X. Yang and A. W. Castleman, Jr., *J. Phys. Chem.* **94**, 8500 (1990).
- ³⁰M. Szcześniak and S. Scheiner, *J. Chem. Phys.* **77**, 4586 (1982).
- ³¹C. McMichael Rohlfing, L. C. Allen, and C. M. Cook, *J. Chem. Phys.* **78**, 2498 (1983).
- ³²S. S. Xantheas, *J. Am. Chem. Soc.* **117**, 10373 (1995).
- ³³L. Tuñón, D. Rinaldi, M. F. Ruiz-López, and J. L. Rivail, *J. Phys. Chem.* **99**, 3798 (1995).
- ³⁴J. J. Novoa, F. Mota, C. Perez del Valle, and M. Planas, *J. Phys. Chem. A* **101**, 7842 (1997).
- ³⁵N. Turki, A. Milet, A. Rahmouni, O. Ouamerli, R. Moszynski, E. Kochanski, and P. E. S. Wormer, *J. Chem. Phys.* **109**, 7157 (1998).
- ³⁶D. Wei, E. I. Proynov, A. Milet, and D. R. Salahub, *J. Phys. Chem. A* **104**, 2384 (2000).
- ³⁷A. R. Grimm, G. B. Bacskay, and A. D. J. Haymet, *Mol. Phys.* **86**, 369 (1995); **87**, 529 (1996).
- ³⁸M. Tuckerman, K. Laasonen, and M. Sprik, *J. Chem. Phys.* **103**, 150 (1995).
- ³⁹M. Tuckerman, K. Laasonen, M. Sprik, and M. Parrinello, *J. Phys. Chem.* **99**, 5749 (1995).
- ⁴⁰M. E. Tuckerman, D. Marx, M. L. Klein, and M. Parrinello, *Science* **275**, 817 (1997).
- ⁴¹P. D. Chong and S. R. Langhoff, *J. Chem. Phys.* **93**, 570 (1990).
- ⁴²A. Rahman and F. H. Stillinger, *J. Chem. Phys.* **55**, 3336 (1971), **57**, 1281 (1972); **61**, 4973 (1974); **60**, 1545 (1974); *J. Am. Chem. Soc.* **95**, 7943 (1973); *Phys. Rev. A* **10**, 368 (1974).
- ⁴³S. V. Shevkunov, P. N. Vorontsov-Velyaminov, and A. A. Martsinovski, *Mol. Simul.* **5**, 119 (1990).
- ⁴⁴P. Ayotte, G. H. Weddle, C. G. Bailey, M. A. Johnson, F. Vila, and K. D. Jordan, *J. Chem. Phys.* **110**, 6268 (1999).
- ⁴⁵J. Kim, S. B. Suh, and K. S. Kim, *J. Chem. Phys.* **111**, 10077 (1999).
- ⁴⁶Y. V. Novakovskaya and N. F. Stepanov, *Int. J. Quantum Chem.* **63**, 737 (1997).
- ⁴⁷P. A. Giguère, *Rev. Chim. Miner.* **20**, 588 (1983).
- ⁴⁸W. R. Busing and D. F. Hornig, *J. Phys. Chem.* **65**, 284 (1961).